Nano Energy 44 (2018) 456–467

Contents lists available at ScienceDirect

Nano Energy

journal homepage: www.elsevier.com/locate/nanoen

Full paper

Superior performances of *in situ* synthesized ZnO/PVDF thin film based self-poled piezoelectric nanogenerator and self-charged photo-power bank with high durability

Pradip Thakur[a,*], Arpan Kool[b,1], Nur Amin Hoque[b], Biswajoy Bagchi[b,2], Farha Khatun[b], Prosenjit Biswas[b], Debdip Brahma[b], Swagata Roy[b], Somtirtha Banerjee[b], Sukhen Das[b]

[a] Department of Physics, Netaji Nagar College for Women, Kolkata 700092, India
[b] Department of Physics, Jadavpur University, Kolkata 700032, India

ARTICLE INFO

Keywords:
PVDF
ZnO
Power density
Self-poled
Self-charged

ABSTRACT

Herein, we have synthesized multitalented β crystallite prosperous and high dielectric ZnO/PVDF thin films via in situ process for energy harvesting and energy storing applications. The impregnation of the ZnO nanoparticles (NPs) in PVDF matrix has enhanced the electroactive β crystal nucleation ($F(\beta)$ ~ 84% at 0.85 vol% doping) as well as piezoelectricity (d_{33} ~ 50 pC/N at 50 Hz) and the dielectric value (~ 109 at 1.7 vol% loading) effectively. The nanogenerator, named as ZPENG and the self-charged photo-power bank (PPB) developed using the optimized supercilious piezoelectric and dielectric films have exhibited superiority in power generation (power density ~ 32.5 mW/cm^3) and energy storage capability (~ 2000 F/) respectively that are highly impressive outputs compare to other similar prototype devices reported elsewhere till now. The realistic utilities of our fabricated ZPENG have been proved by light up 15 serially connected commercial blue light emitting diodes (LEDs) and charging capacitor (1 μF) in a small time span under repetitive finger impartation. The ZPENG is also shows continuous band like power generation under vibration occurred due to blood circulation in human body. The self-charged PPB is also able to power up blue LED that has confirmed its realistic applicability as a power source.

1. Introduction

Recent, energy consumptions and demands of our modern societies are very much increased. The traditional fossils like petroleum, coal etc. are becoming limited to fulfil the energy requirements. And the extraction of electrical energy from traditional fossils are so much linked with recent up-gradation of environmental pollutions as well as the global warming [1–4]. Therefore, the scientists and engineers are deeply involved to overcome this energy demands by developing new clean energy harvesting materials or methods which are capable to harvest energy from the mostly available resources of energy in our living systems (i.e. human movements, solar energy, winds, sea water waves etc.) [4–10]. Few research groups are also associated with fabricating integrated devices which consist both energy harvesting part and storage unit in one hybrid device [4,5,11,12]. Enormous studies have been executed with different materials for developing such types of energy harvesters and integrated devices which consist both energy harvester associated with storage part but the actual achievements are somehow little enough in contrast with modern society demands [11,12].

From the beginning, traditional piezoelectric materials or ceramics like $ZnSnO_3$, PZT, $BaTiO_3$, PMN-PT, and (Na,K)-NbO_3 materials have been used widely for harvesting energy from mechanical energy i.e. for developing piezoelectric nanogenerator (PENG) [13–17]. But the low flexibility and high weight issues of this ceramics quench their versatile utilization in different fields. This limitations are somehow overcome by light weight, highly flexible and cost-effective piezoelectric polymers like poly(vinylidene fluoride) (PVDF) and its copolymers [18,19].

PVDF is a semi-crystalline plastic polymers with five different polymorphs α, β, γ, δ and ε. Non-polar α polymorph (TGTG′ dihedral conformation) is thermodynamically highly stable and melting process directly results in to this phase. The β and γ are mostly popular polar forms of PVDF with TTTT and TTTGTTTG' conformation respectively. Though β, γ and δ are all polar forms of PVDF, but the β polymorph is

* Corresponding author.
E-mail address: pradipthakurju@gmail.com (P. Thakur).
[1] Present address: Department of Physics, Techno India University, Kolkata 700091, India.
[2] Present address: Fuel Cell and Battery Division, Central Glass and Ceramic Research Institute, Kolkata 700032, India.

https://doi.org/10.1016/j.nanoen.2017.11.065
Received 11 October 2017; Received in revised form 21 November 2017; Accepted 28 November 2017
Available online 14 December 2017
2211-2855/ © 2017 Elsevier Ltd. All rights reserved.

most important to the scientist because of its maximum piezoelectric, ferroelectric, pyroelectric and dielectric properties than other phases [19–21]. Thus extensive attempts have been executed by the researchers for improving electroactive β crystal nucleation in PVDF. Electroactive β polymorph crystallization in PVDF has been reported by poling in high electric field [22], electrospinning [23], stretching the α-PVDF film [24] and impregnating with different fillers like metal nanoparticles (NPs) [25], oxide NPs [26], clays [27], carbon nanotube (CNT) [28], salts [19,29], organic molecules [4,5] etc. Impregnation of PVDF with various fillers also increase the dielectric values due to large interfacial polarization and enhancement of dipoles. Both electroactive β phase nucleation and enhancement of dielectric value of doped PVDF film not only opens the possibilities of the materials in energy harvesting industry via piezoelectric property but also energy storage applicability of the materials.

Proper design and configuration of a hybrid device with superior dielectric film which is capable of harvesting of energy from light and stored it in an energy storage part might be able to mould a sustainable energy power pack. Works on hybridization of photovoltaic cells or solar cells with energy storage systems (battery or supercapacitor) are studied extensively for achieving a talented self-charged power pack [30–33]. Prototype integration of solar cells (like perovskite solar cell or dye-sensitized solar cell etc.) with an energy storage parts (like lithium ion battery or supercapacitor etc.) have been fabricated by many research groups [34,35]. This prototype integrations of two different energy harvester and storage unit through external circuits quench the outputs due to increment of overall resistance and lacks in controlling exposure of solar light [36]. Suitable integration of solar light convertor and storage part into one unit may overcome this energy loss issues. Some research efforts have been executed for improving such type of devices [36,37]. Wee et al. fabricated a photosupercapacitor, by integrating an organic photovoltaic (OPV) with CNT based supercapacitor in one unit which reduced internal resistance and power loss [37].

Now days, piezoelectric and dielectric PVDF nanocomposites (NCs) have been utilized for efficient development of PENGs [18,19] and photovoltaically self-charging power unit [4,5]. ZnO nanoparticle (NP) is also a very promising piezoelectric material (piezoelectric coefficient (d_{33}) = 5–12.4 pC/N) and n-type or p-type semiconductor (ΔE = 3.4 eV) nanomaterial for PENG and photovoltaic applications because of their superior biocompatibility, flexibility and easy synthesis method [12,38–39]. Thus, it is widely studied by the scientist for developing energy harvesting from mechanical energy and photovoltaic power systems. By optimizing the doping concentration and uniform distribution of ZnO NPs in PVDF matrix superior piezoelectricity, dielectric value and optical properties may be gained. Though, few researchers designed some prototypes ZnO/PVDF hybrid structures based PENGs and photovoltaic cell but, their poor performances or output characteristics contract their practical utilizations. Jana et al. achieved γ phase nucleation and very low piezoelectricity in ZnO/PVDF (d_{33} = −6.4 pC/N,) [40]. Lee et al. also demonstrate a ZnO nanowire/PVDF based hybrid wearable PENG (output voltage and current-density ~ 0.1 V and 10 nA cm^{-2}) [41]. More recently, Choi et al. has reported a ZnO/PVDF hybrid structure for PENG [42]. PVDF is also used in photovoltaic cells as an energy storage integration. Zhang et al. developed a

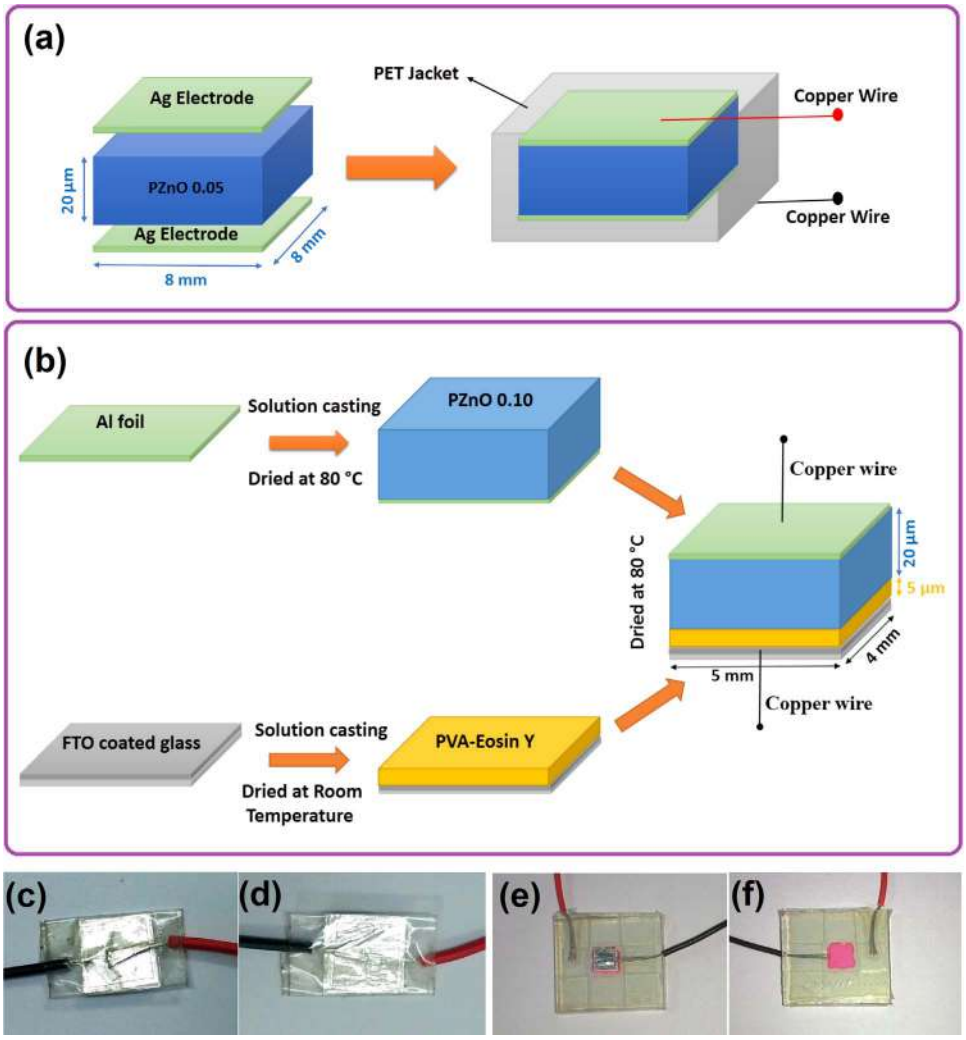

Fig. 1. Schematic diagram of the structure of fabricated (a) ZPENG and (b) self-charged PPB. (c), (d) Digital image of each side of the ZPENG and (e), (f) Digital image of each side of the PPB.

dye-sensitized photovoltaic integrated with storage ability through PVDF/ZnO NCs (energy density $E = 1.4\ \mathrm{mWh\ kg^{-1}}$) [43].

Our present work revolves around the synthesis of flexible ZnO NPs impregnated PVDF thin films with excellent piezoelectricity, dielectric value and optical properties via *In situ* process. Thereafter, two simplistic, cost-effective and highly durable ZnO/PVDF NC thin films seeded prototype devices have been properly demonstrated. One is a piezoelectric nanogenerator cum touch sensor, named as ZPENG (Fig. 1) and another is a self-charging photo-power bank (PPB) (Fig. 1). The self-poled ZPENG and the self-charging PPB proclaim superlative output performances without any external biasing of electricity.

2. Experimental

2.1. Materials

The materials taken are poly(vinylidene fluoride) (Sigma-Aldrich, Germany. M_w: 180 000 GPC, Mn: 71 000), zinc acetate dihydrate ($Zn(CH_3COO)_2{\cdot}2H_2O$)(Sigma-Aldrich, Germany), dimethyl sulfoxide (DMSO) (Merck, India), Eosin Y (EY) (Sigma-Aldrich, Germany), polyvinyl alcohol (PVA) (Loba Chemie, India), FTO coated glass (Sigma-Aldrich, Germany), aluminium foil (Sigma-Aldrich, Germany).

2.2. In situ synthesis of ZnO/PVDF thin films

First, different amount of $Zn(CH_3COO)_2{\cdot}2H_2O$ (0.01, 0.05 and 0.1 M) has been dissolved in 5 mL of 5 mass% PVDF-DMSO solution under continuous stirring for 12 h. Thereafter, the ZnO/PVDF NC thin films are prepared by pouring the whole mixture in petri dishes and drying in a dust oven at 80 °C under ambient pressure. Finally, the ZnO/PVDF thin films of thickness 20 μm have been collected (Named as PZnO 0.01, PZnO 0.05 and PZnO 0.10) and preserved in a vacuum desiccator for further characterization and device fabrication.

2.3. Fabrication of ZPENG

The ZPENG has been designed by taking the PZnO 0.05 thin film with dimension of 8 mm × 8 mm × 20 μm. Silver electrode of 5 μm has been affixed on each side of PZnO 0.05 and two Cu wires are stick out from both electrodes of the PENG for output characteristic measurement purpose. The Cu wires are sealed with the electrodes with the succour of silver paste. Then the whole system is laminated with poly (ethylene terephthalate) (PET) and we grab our desired ZPENG (Fig. 1c and d).

2.4. Development of self-charged PPB

The photo-electrode of our PPB has been prepared by casting 20 μl of EY/PVA solution in water on the FTO. The concentration of EY was 1 mg/mL in 5% PVA solution. When the photo-electrode become sticky, the previously assembled storage electrode containing PZnO 0.10 on aluminium foil (dimension 5 mm × 4 mm × 20 μm) has been put down on it and dried at 60 °C for 1 h for ensuring better connection between the solar and storage part. Finally, two Cu wires plugged by silver paste with both electrode of the PPB have been enlarged out for measuring the performances of the device.

2.5. Characterization and measurement methods

The morphology and microstructures of the samples have been studied by a field emission electron microscope (FESEM) (INSPECT F50, Netherland). Optical properties of the synthesized films are characterized using UV–visible spectrophotometer (Lambda 25, Perkin Elmer, USA and UV −3101PC, Shimadzu) and Cary Eclipse fluorescence spectrophotometer (Agilent Technologies).

Further, the formation of ZnO NPs, investigation of different polymorphs of PVDF and thermal behaviour of the samples have been done utilizing X-ray diffractometer (Model-D8, Bruker AXS Inc, Madison, WI), Fourier transform infrared spectrophotometer (FTIR-8400S,

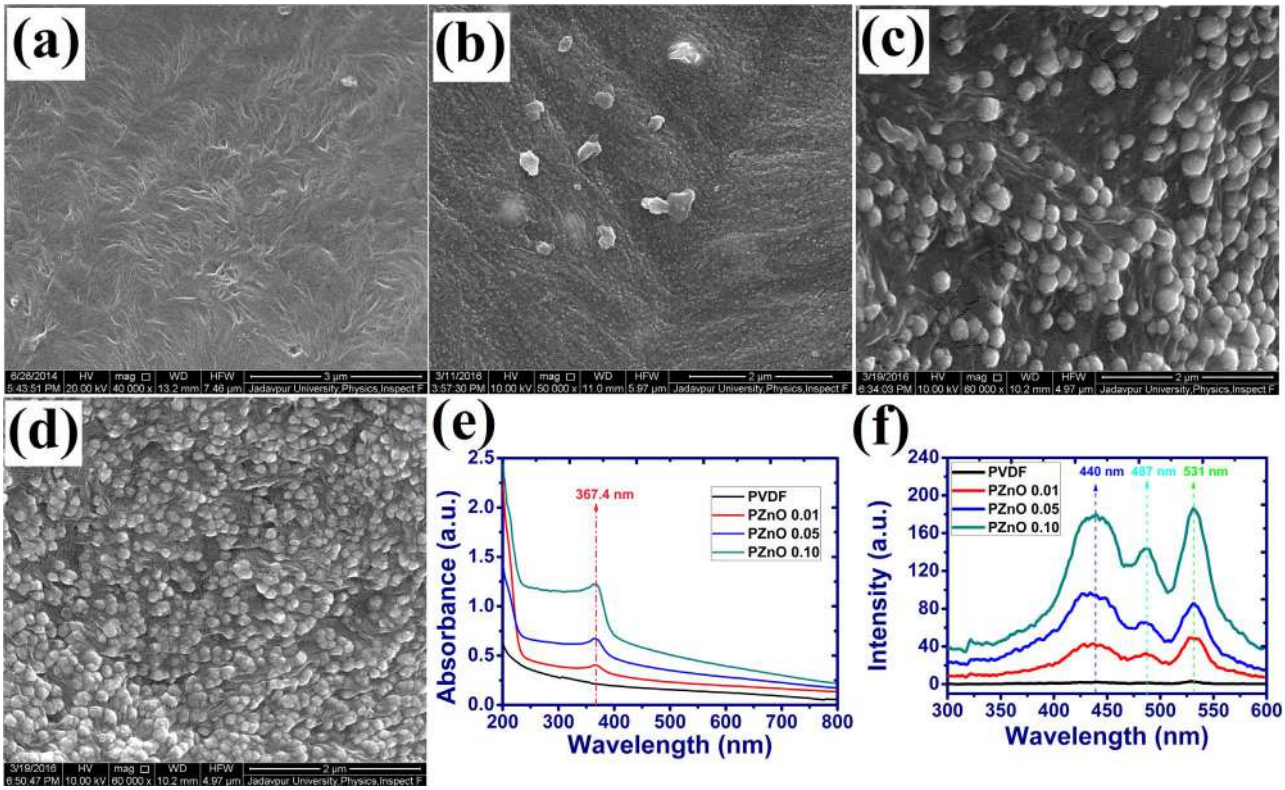

Fig. 2. FESEM images of (a) pure PVDF and (b-d) ZnO NPs loaded PVDF, (e) UV–visible and (f) photoluminescence spectra of pure PVDF and ZnO NPs incorporated PVDF thin films.

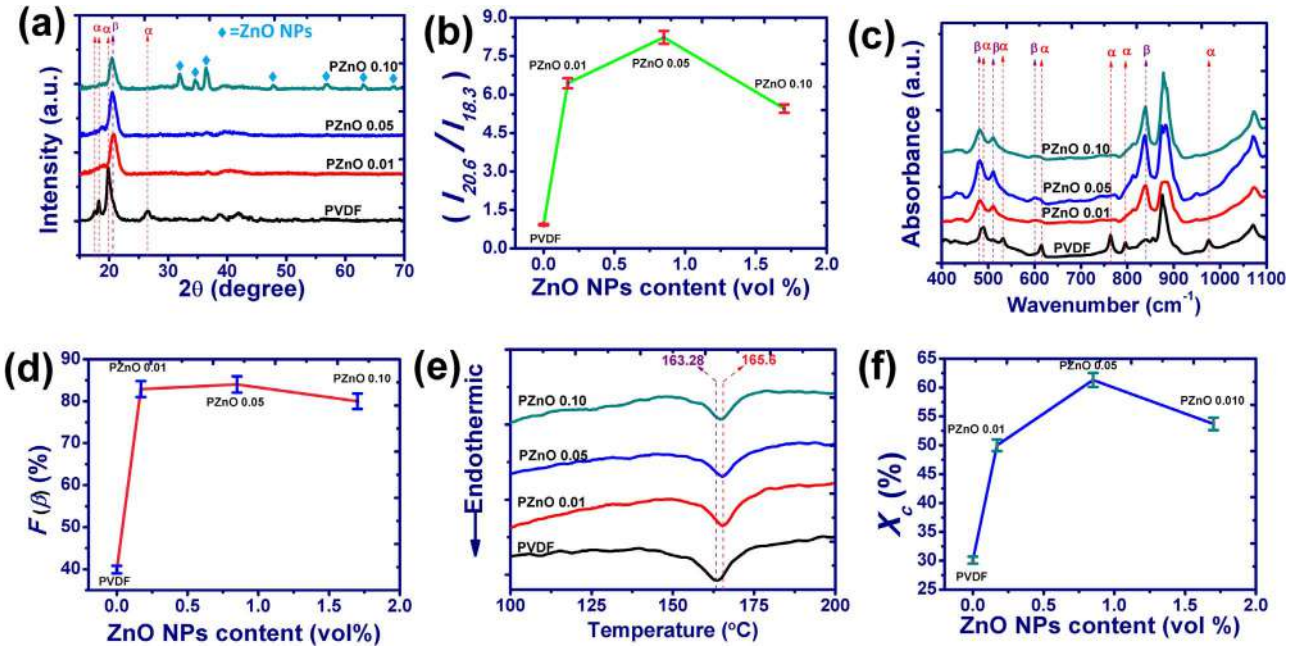

Fig. 3. (a) XRD patterns of unblended PVDF and ZnO/PVDF thin films, (b) Ratio of $I_{20.5}$ and $I_{18.3}$ of the samples calculated from XRD patterns, (c) FTIR spectra of unblended PVDF and ZnO/PVDF thin films, (d) Variation of β-phase content with increasing ZnO NPs concentration evaluated form IR spectra, (e) DSC thermographs of unblended PVDF and ZnO NPs impregnated PVDF thin films and (f) the evaluated degree of crystallinity the samples from DSC thermographs.

Shimadzu), differential scanning calorimeter (DSC-60, Shimadzu (Asia Pacific) Pte. Ltd., Singapore) respectively. Dielectric measurements are carried out recording the capacitance (C) and tangent loss ($tan\delta$) data of the sample under the application of 1 V electric field by a digital LCR meter (Agilent, E4980A). The dielectric constant (ε) and the ac conductivity (σ_{ac}) are evaluated by following formula,

$$\varepsilon = C.\, d/\varepsilon_0 A \tag{1}$$

$$\sigma_{ac} = \omega\varepsilon_0\varepsilon\ tan\delta \tag{2}$$

Here, ε_0, d, A and ω are the permittivity of the free space, thickness of the samples, area of the films and angular frequency applied [4,5].

The performances of ZPENG has been recorded utilizing a digital storage oscilloscope (Keysight, Oscilloscope DSO-X 3012A). And the output characteristics of self-charged PPB are measured by an electrometer (Keysight- B2985A), a digital multi-meter (Agilent U1252A) and cyclic voltammetry technique (PGSTAT 101, Auto Lab).

3. Results and discussions

The design and configuration of two devices, ZPENG and self-charged PPB have been illustrated schematically in Fig. 1a and b respectively and the details fabrication method has been discussed in experimental section. The actual digital photograph of the devices are also demonstrated in Fig. 1c-f. We have used economical and biocompatible ZnO NPs doped PVDF film as effective piezoelectric material for capturing the mechanical energy or small body vibration and converting it into electrical energy. The storage capability of the ZnO-PVDF NC film also successfully investigated by designing an integrated solar power cell consisting this ZnO NPs induced high dielectric polymeric thin film as storage function. Our study resolves around the designing and characterization of ZnO-PVDF film for their optimal practical utilization not only in the field of energy conversion or sensors but also energy storage field.

3.1. Characterization and specification of ZnO-PVDF films for devices

3.1.1. Morphology and microstructure

Fig. 2a-d illustrated the morphological and structural micrograph of the surfaces of unblended PVDF and the ZnO NPs modified PVDF films respectively. Uniform in situ growth of spherical ZnO nanostructure (average diameter ~ 50–150 nm) have been observed throughout the all NC samples. The average diameter of the ZnO NPs seems to be reduced with increasing concentration of the salt enhancing their effective surface area and the negative charge distribution density (Illustrated in Supporting information Fig. S1). This increment of surface area of the in situ ZnO NPs lead to intimal interaction and well distribution all over the PVDF matrix.

3.1.2. Optical properties

Optical properties i.e. light absorption and emission properties of the ZnO-PVDF NC thin films are studied and depicted in Fig. 2e and f respectively. The UV–visible absorption spectra of ZnO-PVDF samples are associated with a strong absorption peak at ~ 364.7 nm (E~ 3.4 eV) asserting the evaluation of ZnO NPs in the composite samples, whereas pure PVDF represents no such characteristic absorption band. Also, the overall intensities of the absorbance spectrum for NC samples are enhanced with the raise of impregnation of the polymer sample with ZnO NPs which indicates uniform distribution and interaction of the NPs with PVDF chains. Thus, ZnO-PVDF film may be applied effectively for shielding or sensing UV-A light. Fig. 2f demonstrates the photoluminescence emission characteristics of unblended PVDF and ZnO NPs impregnated PVDF thin films [44,45]. Three prominent emission bands are appeared centring around 440 nm, 487 nm and 531 nm upon excitation of the ZnO NPs incorporated PVDF films with wavelength λ_{ex} = 235 nm. Whereas, no characteristic emission bands have been shown in the unblended PVDF film at equal excitation. The NC samples may also be used to develop the next generation polymeric light emitting diodes, UV driven photovoltaic cells and optoelectronics due to their superior visible light emission ability.

3.1.3. Investigation and quantification of electroactive β crystallite

Effective nucleation of electroactive β crystallite in the NPs modified PVDF films have been confirmed from XRD, FTIR and DSC studies. Fig. 3a and b represent the XRD pattern of the unblended and NPs doped PVDF films and the calculated quantities of β polymorph from XRD spectra respectively. The XRD spectrum of pure PVDF consists of

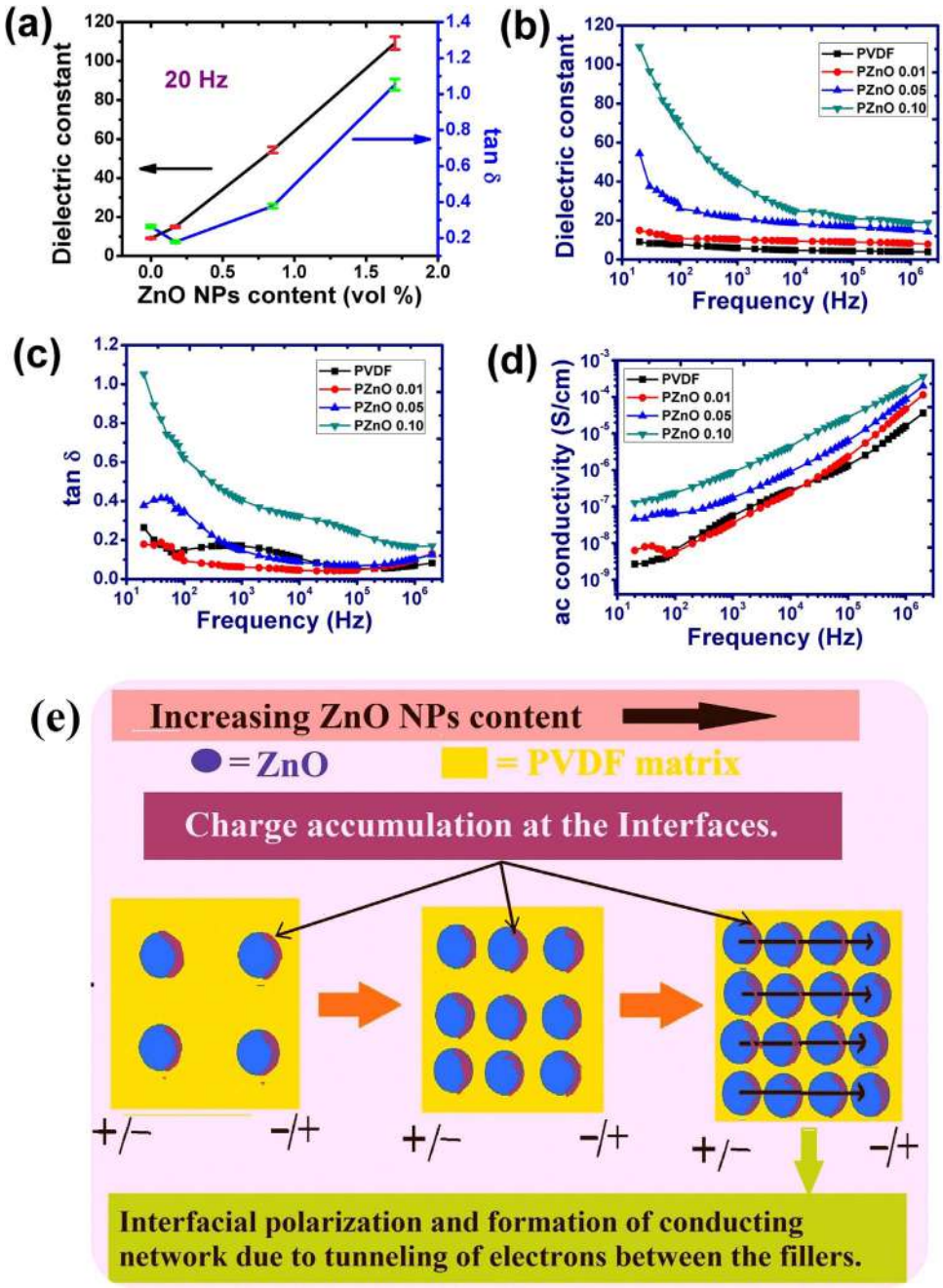

Fig. 4. (a) Variation of dielectric constant and tangent loss of unblended PVDF and ZnO/PVDF films with ZnO NPs content. Dependency of (b) dielectric constant, (c) tangent loss and (d) ac conductivity with frequency. (e) Schematic representation of the formation conducting networks and interfacial charge accumulation in ZnO/PVDF films.

the characteristic peaks of nonpolar α crystal at 2θ = 17.5°, 18.3°, 19.9° and 26.4° (Fig. 3a) [4,19,20]. In the diffraction patterns of the NC samples, the characteristic peak of the electroactive β crystallite (at 2θ = 20.6°) appeared prominently diminishing all peaks associated with nonpolar α crystal [19,20]. Additional diffraction peaks at 2θ = 31.9° (100), 34.5° (002), 36.3° (101), 47.7° (102), 56.74° (110), 63.0° (103) and 68.1° (112) are also noticed for PZnO 0.10 which corresponds to the characteristic peaks of ZnO NPs (Fig. 3a) [46]. The ratio of the intensities of the peaks at 20.6° and 18.3° ($I_{20.6}/I_{18.3}$) have been calculated for all samples for qualitative illustration of the quantity of α and β crystals in the samples and the values are depicted in Fig. 3b. The value of the $I_{20.6}/I_{18.3}$ are higher than that of pure PVDF (~0.93) and reached highest ~ 8.23 for 0.85 vol% ZnO NPs incorporation (PZnO 0.05) [20]. The result infers highest β polymorph nucleation in PZnO 0.05.

The FTIR analysis of the samples further confirms the nucleation of electroactive β phase nucleation in the ZnO NPs modified PVDF samples (Fig. 3c and d). The IR spectrum of unblended PVDF fully consists of the characteristics absorbance bands of α crystals at 490 cm^{-1} (waging of CF_2 bond) 531.5 cm^{-1} (CF_2 bonds bending), 615 and 765 cm^{-1} (CF_2 skeletal bending), 796 and 975 cm^{-1} (CH_2 rocking). Incorporation of ZnO NPs in PVDF matrix leads to complete suppression of α crystal characteristic peaks. Raising of absorbance bands at 479 cm^{-1} (CF_2 deformation), 510 cm^{-1} (CF_2 stretching), 600 cm^{-1} (CF_2 wagging) and 840 cm^{-1} (CH_2 rocking, skeletal C–C and CF_2 stretching) are spotted in the ZnO/PVDF films which validates the β crystallite formation [4,5,20]. Evaluation of electroactive β crystal content ($F(\beta)$) in the samples are executed using Lambert–Beer law,

$$F(\beta) = \frac{A_\beta}{\left(\frac{K_\beta}{K_\alpha}\right)A_\alpha + A_\beta} \quad (3)$$

Here, A_α and A_β are the absorbance intensities at 765 cm^{-1} and

840 cm^{-1}, $K_\beta = 7.7 \times 10^4\ cm^2\ mol^{-1}$ (the absorption coefficient at 840 cm^{-1}) and $K_\alpha = 6.1 \times 10^4\ cm^2\ mol^{-1}$ (the absorption coefficient at 764 cm^{-1} [4,21]. The evaluated $\boldsymbol{F(\beta)}$ are graphically represented in Fig. 3d. Maximum 84% for 0.85 vol% impregnation of in situ ZnO NPs in polymer matrix (PZnO NPs) which is compatible with XRD analysis of the samples.

The thermal stability and the crystalline behaviour of the samples are also verified using thermal gravimetric analysis and DSC data which are presented in Fig. S2 (See Supporting information) and Fig. 3e respectively. Incorporation of ZnO NPs in PVDF hikes the thermal decomposition temperature of the NC samples by 25 °C than the unblended one (Fig. S2). The DSC thermographs demonstrate the shifting of melting temperature values to higher temperature by ~ 2.3 °C in the thermograph of ZNO/PVDF film inferring β polymorph crystallization in the samples [4,5]. The melting enthalpy values (ΔH_m) and degree of crystallinity (X_c) are also seemed to raise with ZnO NPs loading in the polymer matrix (See Fig. S3 I Supporting information and Fig. 3f). The X_c value reached maximum ~ 64.1% for 0.85 vol% incorporation of NPs due to highest longer alignment of polymer chains in *all trans* i.e. TTTT conformation at that concentration of doping. The X_c has been calculated according to equation, $X_c = \Delta H_m / \Delta H_{100\%}$, (where, $\Delta H_{100\%}$ = 104.6 J/g, the melting enthalpy of 100% crystalline PVDF) [19,20]. The negatively charged ZnO NPs have conducted optimum catalytic effect for nucleation of polar β spherulites in PVDF at very low loading of the NPs (0.85 vol%). Furthermore loading of NPs in polymer matrix contracts the chain movements of the PVDF resulting fall in crystallinity values as well as the β polymorph nucleation.

Thus, we get the desired electroactive β polymorph prosperous ZnO/PVDF thin film named as "PZnO 0.05" for PENG fabrication as well as for touch sensor application. The piezoelectric coefficient (d_{33}) of the PZnO 0.05 sample also verified and the d_{33} value is found to be 50 pC/N at 50 Hz (See Supporting information for measurement details) [47]. The highest nucleation of β crystallite in PZnO 0.05 and the combine synergetic effect of both piezoelectric ZnO NPs and β crystallite pilots to superior d_{33} value of the sample.

3.1.4. Dielectric properties

Dielectric properties of the unblended PVDF and ZnO/PVDF film have been thoroughly examined. The dielectric properties i.e. dielectric constant, tangent loss and the conductivity behaviours of the samples are very much dependent on the β phase content and the interfacial polarization occurred in the samples due to impregnation by the ZnO NPs. Here Fig. 4a demonstrates the variation of dielectric constant and associated tangent loss with dopant concentration i.e. ZnO NPs content in polymer matrix at 20 Hz. The dielectric constant is improved linearly with ZnO NPs doping concentration and it reaches highest value ~ 109 at 1.7 vol% incorporation of the NPs (PZnO 0.10) where the dielectric constant of unblended PVDF is ~9 at same frequency. The tangent loss is also very low, it is just ~1.05. It is noted that incorporation of ZnO NPs improves the dielectric constant by 12 times than that of pure PVDF, whereas the tangent loss is increased by only 4 times than the loss value of unblended one. Fig. 4b-d illustrate the dependency of dielectric properties i.e. dielectric constant, tangent loss and ac conductivity with increasing frequency. Though the dielectric constant has been decreased with increasing frequency for all samples (Fig. 4b) but the values have been still followed the increasing characteristic with NPs content throughout whole frequency range (20 Hz to 2 MHz). The tangent values are also changed with similar fashion like dielectric constant all over the measured frequency range. Whereas the ac conductivity has been linearly increased with applied frequency. The

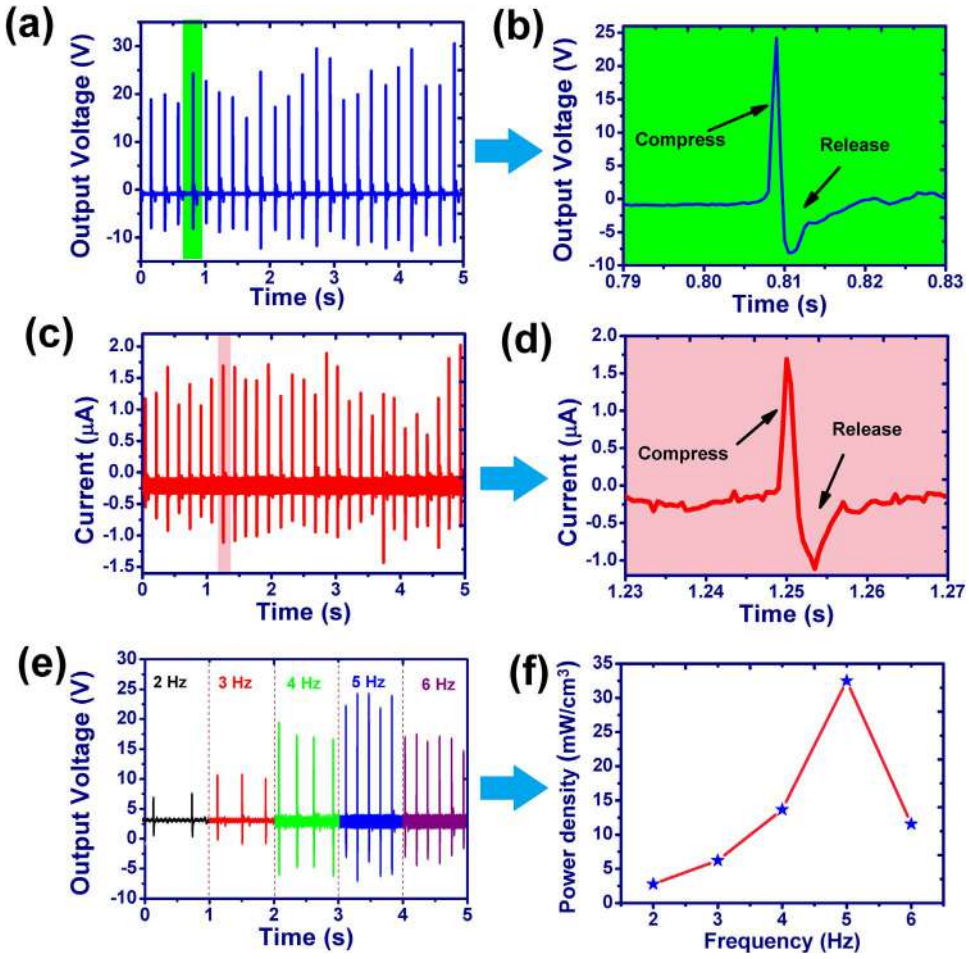

Fig. 5. (a, c) The open-circuit voltage (V_{oc}), and short-circuit current (I_{sc}) under periodic finger impartation and relaxation by the ZPENG, (b, d) the open-circuit voltage (V_{oc}), and short-circuit current (I_{sc}) due to single finger impartation and relaxation, (e) Dependency of applied force frequency of the output voltage generated by ZPENG and (f) Variation of power density produced by the ZPENG at different frequency of applied force.

conductivity characteristic of all samples are purely ac type, there is no presence of dc conductivity region. The interaction of ZnO NPs with polymer chains and the charge accumulation of charge carriers in the interfaces between the NPs and the PVDF chains are schematically depicted in Fig. 4e. As the NPs surface charge is negative, these interacts with the positive $-CH_2$ dipoles of the polymer matrix via ion-dipole interaction or electrostatic attraction. This uniform ion-dipole interaction between the NPs and polymer chains effectively increased the polar β phase content in ZnO/PVDF film. Though the main factor behind the enhancement of dielectric properties of the film is the

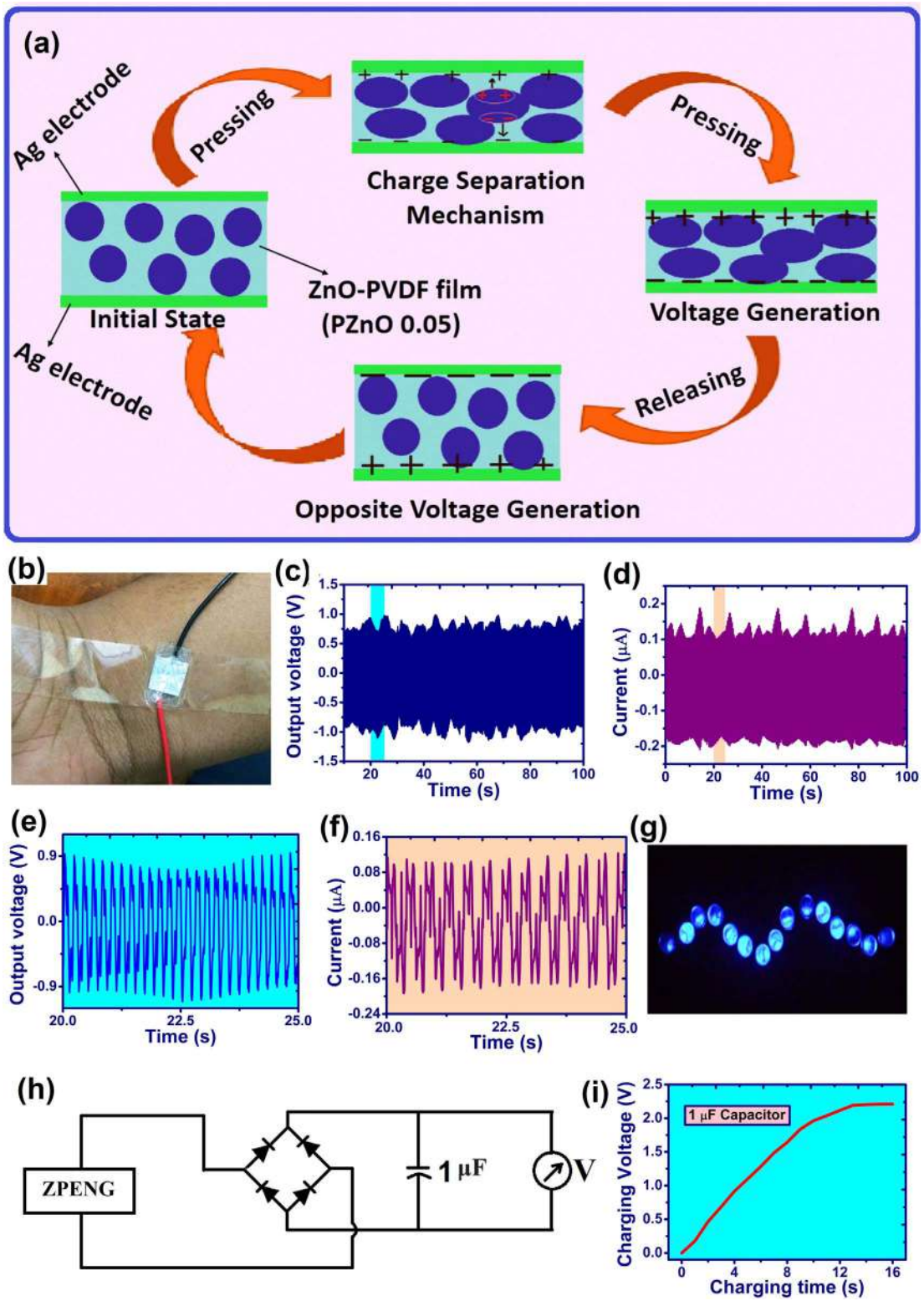

Fig. 6. (a) Schematic working mechanism of the ZPENG under applied force due to piezoelectric responses of the PZnO 0.05 sample, (b) Digital photograph of attachment of the ZPENG on the hand, (c, d) the Band like output voltage and current under touching condition of the device on the hand, (e, f) the magnified image of the band like output voltage and the current when placed on the hand, (g) Snapshot of the lighting of commercial blue LEDs driven using our ZPENG under periodic finger impartation, (h) Circuit diagram of capacitor charging and (i) Charging characteristic or voltage-time graph of 1 μF capacitor using our ZPENG.

Maxwell–Wagner–Sillars (MWS) interfacial polarization occurred at the interfaces between the ZnO NPs and PVDF chains, the dipolar polarization due to the dipole alignment in TTTT conformation i.e. β crystallites also contribute to increase the dielectric value. The MWS effect has appeared within a heterogeneous system of phases with non-identical conductivity via accumulation of charges at the interfacial surfaces [20,26,48,49]. Here, the interfacial polarization via MWS effect has been increased with increasing ZnO NPs impregnation into the PVDF [26,48]. The inter-particle distances among the ZnO NPs are also decreased with the increment of doping content. When the loading concentration of ZnO NPs reaches to a certain characteristic value i.e. the percolation value of the composite that is 1.7 vol%, the dielectric constant value has become maximum which may be due to the formation of conducting network through the tunnelling of electrons from one ZnO NP surface to its closer ZnO NP (Fig. 4e) [26,48,49]. Here, we obtained a high dielectric PZnO 0.10 film with low loss and this dielectric film is utilized for storing the electrical charge in our prototype high performing simplistic self-charged PPB.

3.2. Output characteristics and realistic utilization of the ZPENG

The simplistic PENG has been fabricated using the most piezoelectric ZnO/PVDF film that is "PZnO 0.05" with d_{33} value ~ 50 pC/N at 50 Hz (Table S1). The output characteristics i.e. the open circuit output voltage (V_{oc}) and the short circuit current (I_{sc}) have been demonstrated applying continuous finger impartation and relaxation conditions at an approximate mechanical force ~ 28 N (see Supporting information) with frequency~ 5 Hz. The ZPENG is highly sensitive to human pressure which is illustrated later and the performances are much better than the unblended PVDF film. The output characteristics of the ZPENG under periodic finger impartation have been illustrated in Fig. 5. The ZPENG builds open circuit voltage (V_{oc}) ~ 24.5 V and short circuit current (I_{sc}) ~ 1.7 μA which leads to very high power density of ~ 32.5 mW/cm^3 (Fig. 5a-d). The d_{33} value of the PZnO 0.05 film is well consistent with the output characteristic i.e. superior performances of our fabricated ZPENG (See the Supporting information). The performances of our fabricated ZPENG are much better than previously reported ZnO/PVDF based PENG as well as other PENGs that have been studied under same conditions [47]. Comparative performances of our

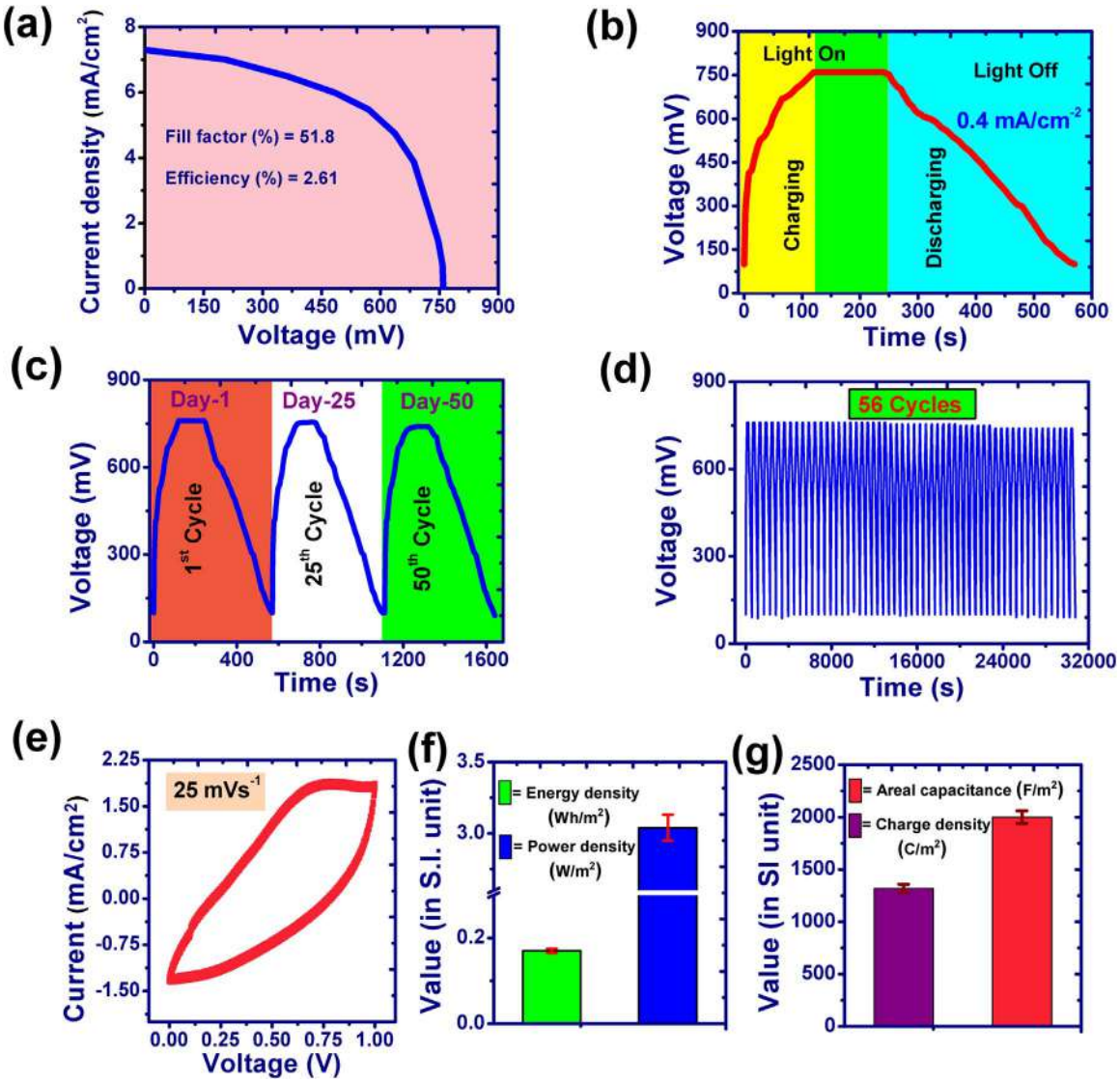

Fig. 7. (a) J-V characteristic of our self-charged PPB under light illumination, (b) Self-charging and discharging curve as a function of time i.e. *V-t* graph of the PPB under light on and off condition, (c, d) Repetitive charging-discharging characteristic (*V-t* graph) of the device under light on and off condition, (e) cyclic voltammetry curve with 0–1 V at 25 mV/s voltage change, (f) Calculated energy density and power density from the discharging *V-t* curve (discharged under constant current = 0.4 mA/cm^2) and (g) Evaluated charge density and areal specific capacitance of our PPB in fully charged condition.

ZPENG with other PENGs reported elsewhere are shown in Table S2, S3 and S4 (Supporting information). The performances of our ZPENG with varying frequency under constant force (~28 N) have also been examined and presented in Fig. 5e. Fig. 5f illustrates the changes of power density of the ZPENG with varying frequency of the repetitive constant finger impartation (~28 N). Maximum performances have been pointed out at 5 Hz frequency. The durability test i.e. the recycle performances of our ZPENG are also examined for 8 weeks (one cycle of 500 s per week). The performances are retained similar even after this long duration (~2 months) shown in Fig. S5 (See Supporting information).

Fig. 6a represents electrical voltage generation mechanism under periodic finger impartation and relaxation schematically. The generation of electrical signal under mechanical force may be explained in terms of the combine piezoelectric effect due to the polar dipoles in the PVDF and the piezo-effect of ZnO NPs. The impregnation of negatively surface charged ZnO NPs reinforces the piezoelectric or electroactive β crystallites in PVDF thin film. When the ZnO/PVDF film has been imparted, the film is self-polarized due to dual piezoelectric effect of β crystallites and the ZnO NPs. The additional electrical charge separation in piezoelectric ZnO NPs due to slight changes in their shapes also trigger alignment of polymer chains in *all trans* conformation. Thus, the synergetic electrical charge generation effect by the electroactive or piezoelectric β crystals and the ZnO NPs in combine generates superior output electrical signal in between the two silver electrodes. Under vertical mechanical pressing, the positive piezoelectric charge has been gathered on top electrode whereas the bottom one has been induced by same amount of negative piezoelectric charge. Thus a piezoelectric potential has been occurred between the two electrode and the electron flows from one electrode to other across an external load without any external bias. When the impartation is withdrawn i.e. at pressure relaxation condition, the potential due to piezoelectricity has been diminished rapidly and the electrons are migrated to the opposite electrode through external circuit and accumulated there. Thus an opposite potential drop has been produced in between the two electrodes at relaxation condition [19,47]. This separation and migration of the charge carriers i.e. electrons are simply illustrated in Fig. 6a.

The superior performances i.e. power density and recyclability are the basic key point of our prototype ZPENG for practical utilization. The realistic utilization of the device is studied through examining its human body vibration sensitivity, glowing of commercially available light emitting diodes (LEDs) and the charging capability of storage gadgets like capacitor.

First, the performances of our device under small pressure due to human body vibration i.e. vibration produced due to blood circulation in our body has been investigated and illustrated in Fig. 6b-f. The ZPENG has been placed in contact with skin of human hand (Fig. 6b) and the generated output characteristics (open circuit voltage and short circuit current) due to pressure impartation on the device by body vibration are collected. Continuous band like open circuit voltage (V_{oc} ~ 1 V) and short circuit current (I_{sc} ~ 0.15 μA) are produced under the body vibration (Shown in Fig. 6c-f). This output characteristics are very much interesting and this results open the application possibilities of the device in the field of bio-medical for monitoring pressure and heart beat as well as in the portable appliances like mobiles for charging under body contact (See comparison Table S5 in Supporting information). Further, the realistic usage and energy generation ability of our PENG has been demonstrated by driving the LEDs. Our prototype ZPENG is efficient to light up 15 blue LEDs connected serially under periodic finger impartation shown in Fig. 6g. The output voltage is rectified by a full wave rectifier for lighting the LEDs. The superiority of our ZPENG for charging a capacitor (1 μF) has also been examined (Fig. 6h and i). The capacitor charging circuit connection is shown in Fig. 6h. The device is able to charge the capacitor (upto ~2.2 V) only in 13 s under periodic finger impartation and relaxation condition illustrated in Fig. 6i that is very promising compare to previous prototype PENG reported elsewhere (See comparison Table S6 in Supporting information).

3.3. Performances of the self-charged PPB and its storage mechanism

The low loss high dielectric "PZnO 0.10" thin film is utilized as an efficient energy storage part in our simple prototype self-charged PPB consisting EY/PVA film as solar energy absorber and converter unit shown schematically in Fig. 1b. Fig. 7a presents the current density (J)-voltage (V) characteristic of the self-charged PPB under 110 mW/cm^2 illumination with the help of a 40 W tungsten bulb combined with UV and IR blocking filters. Fabrication of two electrode hybridized power cell consisting both light conversion part and storage part in one unit is very challenging as incorporation of energy storage part in to a photovoltaic dramatically reduced the overall power conversion efficiency (*PCE*). The poor PCE of such hybridized devices have limited their practical utilization possibilities. Our self-charged PPB exhibits a good PCE of 2.61% with the open circuit voltage (V_{oc}) of 760 mV, short circuit current density (J_{sc}) of 7.3 mA/cm^2 and fill factor (*FF*) of 0.518 that exposes its realistic application possibilities. Fig. 7b presents the self-charging and discharging characteristic of our PPB under light irradiation (P_{in} = 110 mW/cm^2). The PCE and the FF have been evaluated using the equations,

$$PCE = V_{oc}.\ J_{sc}.\ FF/P_{in} \quad (4)$$

$$FF = V_{mp}.\ J_{mp}/V_{oc}.\ J_{sc} \quad (5)$$

Here, V_{mp} and J_{mp} are the voltage and current at maximum power point of the PPB determined from *J-V* curve [45].

The PPB is fully charged to 760 mV under light exposure within 120 s in open circuit situations and this photovoltage is retained well in the PPB. The discharging process of the device is therefore investigated with a constant discharge current density of 0.4 mA/cm^2. The photovoltage is slowly discharged to its initial value by 330 s. The recycling performances of the PPB has also been verified over 56 days (1 cycle per day) by simultaneous charging-discharging process shown in Fig. 7c and d. The photovoltage value is reduced only by 2.6% after 56 cycles i.e. 56 days.

The electrochemical behaviour of the self-charged PPB has been examined using cyclic voltammetry (CV) measurement. Fig. 7e shows the CV curve of our PPB measured in a potential window of 0–1 V at a scan rate 25 mV/s. The rectangular shape of the CV curve of our fabricated self-charged PPB have illustrated the super-capacitive nature of the power bank.

Further, the energy storage density (E_A), power density (P_A), stored charge density (Q_A) and areal specific capacitance (C_A) have been calculated *V-t* charging-discharging graph (Fig. 7b) according to the following equations,

$$E_A = 0.5 C_A V^2 \quad (6)$$

$$C_A = \left(\int I_A.\ dt\right)/dV \quad (7)$$

$$Q_A = \int I_A.\ dt \quad (8)$$

$$P_A = V.\ I_A \quad (9)$$

Here, I_A = the constant discharge current (0.4 mA/cm^2), dV = discharge potential difference and V = maximum voltage [50–52].

The stored energy density of the self-charged PPB has been evaluated to be 0.17 Wh/m^2 with power density of 3.04 W/m^2 depicted in Fig. 7f. The areal specific capacitance are found to be 2000 F/m^2 with charge density of 1320 C/m^2 illustrated in Fig. 7g. The measured areal specific capacitance as well as other storage characteristics (i.e. energy density, power density or charge density) of our PPB are notably striking results in the field of hybrid self-charging photo induced energy storage devices i.e. photo-supercapacitors and this output characteristics are so much challenging to other prototype integrated photovoltaic cells associated with energy storage function reported elsewhere (See comparative Table S7 in Supporting information) [4,5,43,50–52].

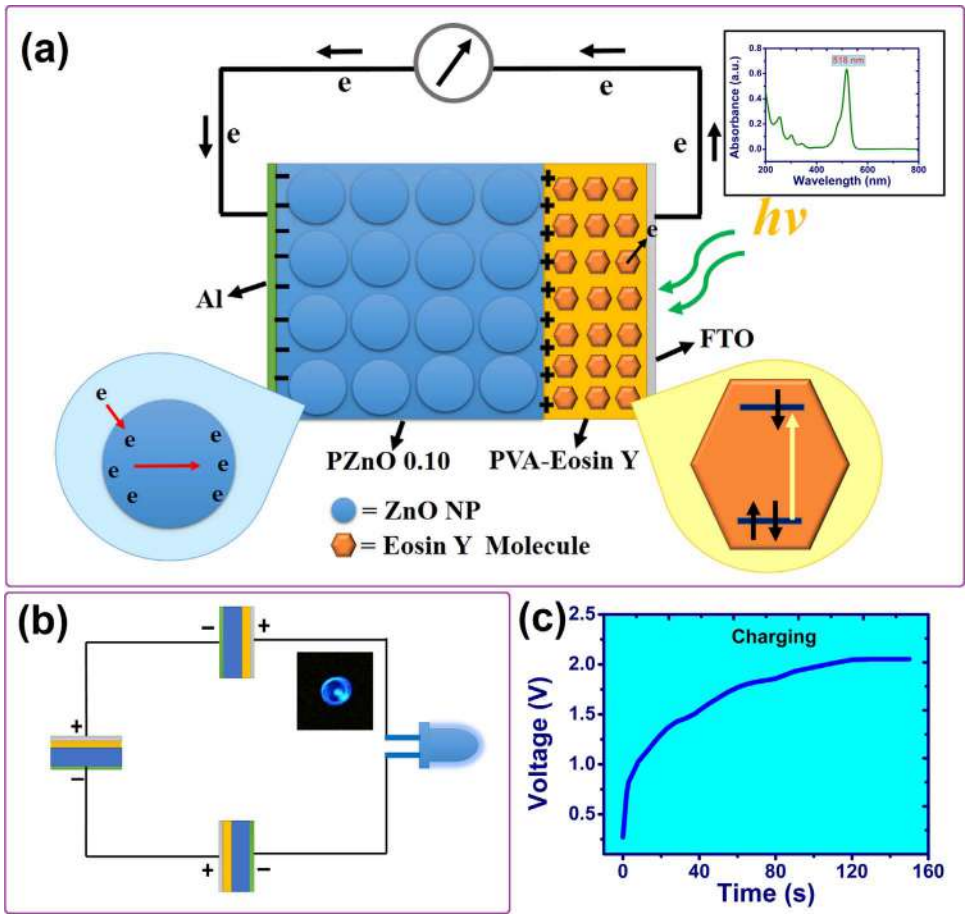

Fig. 8. (a) Schematic presentation of the photoelectrons generation and their storage mechanism in the PPB under exposure of light (Inset shows the UV–visible spectrum of EY/PVA thin film), (b) Schematic Photo-charging circuit diagram of serially connected by which a blue LED is driven using the three PPB as power source and (c) The photo-charging curve (V-t graph) of three serially connected PPB under light.

Further, the photoelectrons generation absorbing the light and their storage mechanism in the device have been explained in detail and the possible mechanism has been demonstrated schematically in Fig. 8a. The electron creation and storage process are somehow very similar and simple like our previously reported self-charging photovoltaic cells with energy storage function. In present prototype device, when the photon absorbing electrode i.e. FTO-EY/PVA are illuminated under light, photoelectrons are generated by the EY dye [53,54]. The EY molecules have absorbed the photons of visible light ($\lambda \sim 518$ nm shown in inset of Fig. 8a) and produce the electrons which moves to the adjoining conducting FTO [54]. The photoelectrons are further migrated from FTO to the conducting Al electrode through connecting Cu wire and stored at the adjacent between the Al and PZnO 0.10 film as well as at the interfaces of ZnO and PVDF chains. At the similar time, the electrons vacancy in EY molecules are filled up by the donation of electrons from PVA molecules. Thereafter, the EY molecule again absorbs light and generates electrons which are migrated to the counter electrode and stored in the dielectric "PZnO 0.10" film. This process has been repeated and the photogenerated electrons in acting electrode i.e. FTO-EY/PVA are stored in counter electrode containing the storage part "PZnO 0.10". So, a photovoltage has been developed due to separation of charges (i.e. holes and electrons) on the either side of the dielectric film. Here the photogenerated potential difference between the two electrodes also act as the self-driving force or bias for energy storage in the PPB [4,5,43]. The movement of photoelectrons and their storage in "PZnO 0.10" film are simplified in schematic diagram (Fig. 8a). An energy state diagram indicating different energy levels in vacuum of the active materials of our PPB are depicted in Fig. S7 (See Supporting information). The energy state diagram well supports the flow of the photoelectrons from acting electrode to counter electrode via adjoining Cu wire.

Further, the realistic utilization of our self-charged PPB has been demonstrated by lighting up the commercially available LED using the three serially connected PPB as power unit (Fig. 8b). The serially connected three PPBs are self-charged up to 2 V within 2 min and that combine power unit are able to drive a blue LED constantly for 6 s (See Video S2 supplied as Supporting information). Thus, the superior performances of our prototype self-charged photo-power unit demonstrates itself as a promising prospect for the partial fulfilment of energy consumptions of our modern electronics gadgets.

Supplementary material related to this article can be found online at http://dx.doi.org/10.1016/j.nanoen.2017.11.065.

4. Conclusions

In summary, we have fabricated two simple ZnO-PVDF film based prototype energy harvesting unit able to harvest electrical energy from two mostly available clean resources of our living system and nature with superior performances. The nanogenerator (ZPENG) reveals to superior and enhanced output characteristics ($V_{oc} \sim 24.5$ V and $I_{sc} \sim 1.7$ μA) associated with a remarkable power density ~ 32.5 mW/cm^3 under periodic finger impartation with long durability or recyclability. Our ZPENG is also capable to generate constant power band with average power density ~ 0.12 mW/cm^3 ($V_{oc} \sim 1$ V and $I_{sc} \sim 0.15$ μA) capturing the small human body vibration due to blood circulation. The capacitor (1 μF) charging efficiency (~ 2.2 V) in a short span of time (~ 13 s) and the ability of power up the serially connected LEDs have proved the realistic applicability of our ZPENG. Further, our fabricated self-charged PPB also shows its efficient performances compare to other hybrid photo-supercapacitors i.e. photovoltaic cells with storage function reported elsewhere till date. The PPB exhibits good PCE $\sim 2.61\%$ with efficient charge and energy density of 1320 C/m^2 and 0.17 Wh/m^2

respectively. The areal specific capacitance of fully charged PPB is found to be 2000 F/m^2 with maximum power density of 3.04 W/m^2. Most importantly, our PPB shows excellent power creation capability over a long periods (8 weeks). The practical utilization is also affirmed by driving a blue LED using the PPB as power source. Thus, our study provides two powerful and cost-effective prototype ZnO-PVDF based devices for the development of next generation superior renewable energy harvester from mechanical energy, biomedical kits and self-charged photon induced self-charged power bank for daily life utilizations.

Acknowledgements

Authors are thankful to University Grants Commission (UGC), India, (F. 17-76/2008 (SA-1)) for providing funds.

Supporting information

The surface charge of ZnO NPs analysis, thermal gravimetric thermographs of the samples, Frequency dependency of output characteristics of ZPENG, "calculation of power density, imparting force and piezoelectric characteristic", energy diagram of active materials used in PPB and comparative performances tables are supplied as supporting information file.

Demonstration of glowing of LEDs by ZPENG and PPB supplied as Video S1 and Video S2 file.

Appendix A. Supplementary material

Supplementary data associated with this article can be found in the online version at http://dx.doi.org/10.1016/j.nanoen.2017.11.065.

References

[1] G.J. Aubrecht, Energy: Physical, Environmental and Social Impact, 3rd ed., Pearson, Upper Saddle River, NJ, 2006.
[2] S. Chu, A. Majumdar, Nature 488 (2012) 294–303.
[3] E.A. Rosa, T. Dietz, Nat. Clim. Change 2 (2012) 581–586.
[4] F. Khatun, N.A. Hoque, P. Thakur, N. Sepay, S. Roy, B. Bagchi, A. Kool, S. Das, Energy Technol. 5 (2017) 1–12.
[5] S. Roy, P. Thakur, N.A. Hoque, B. Bagchi, N. Sepay, F. Khatun, A. Kool, S. Das, ACS Appl. Mater. Interfaces 9 (2017) 24198–24209.
[6] X. Wang, J. Song, J. Liu, Z.L. Wang, Science 316 (2007) 102–105.
[7] J. Chen, J. Yang, H. Guo, Z. Li, L. Zheng, Y. Su, Z. Wen, X. Fan, Z.L. Wang, ACS Nano 9 (2015) 12334–12343.
[8] L. Gu, N. Cui, L. Cheng, Q. Xu, S. Bai, M. Yuan, W. Wu, J. Liu, Y. Zhao, F. Ma, Y. Qin, Z.L. Wang, Nano Lett. 13 (2013) 91–94.
[9] J. Liu, N. Cui, L. Gu, X. Chen, S. Bai, Y. Zheng, C. Hu, Y. Qin, Nanoscale 8 (2016) 4938–4944.
[10] W. Yang, J. Chen, G. Zhu, J. Yang, P. Bai, Y.J. Su, Q.S. Jing, X. Cao, Z.L. Wang, ACS Nano 7 (2013) 11317–11324.
[11] A. Ramadoss, B. Saravanakumar, S.W. Lee, Y.S. Kim, S.J. Kim, Z.L. Wang, ACS Nano 9 (2015) 4337–4345.
[12] Q. Zhang, C.S. Dandeneau, X. Zhou, G. Cao, Adv. Mater. 21 (2009) 4087–4108.
[13] J.M. Wu, K.H. Chen, Y. Zhang, Z.L. Wang, RSC Adv. 3 (2013) 25184–25189.
[14] K.-I.P. Park, J.H. Son, G.T. Hwang, C.K. Jeong, J. Ryu, M. Koo, I. Choi, S.H. Lee, M. Byun, Z.L. Wang, K.J. Lee, Adv. Mater. 26 (2014) 2514–2520.
[15] Z.H. Lin, Y. Yang, J.M. Wu, Y. Liu, F. Zhang, Z.L. Wang, J. Phys. Chem. Lett. 3 (2012) 3599–3604.
[16] S. Xu, Y.W. Yeh, G.P. Poirier, M.C. McAlpine, R.A. Register, Y. Nan, Nano Lett. 13 (2013) 2393–2398.
[17] H.B. Kang, J. Chang, K. Koh, L. Lin, Y.S. Cho, ACS Appl. Mater. Interfaces 6 (2014) 10576–10582.
[18] C. Chang, V.H. Tran, J. Wang, Y.K. Fuh, L. Lin, Nano Lett. 10 (2010) 726–731.
[19] N.A. Hoque, P. Thakur, S. Roy, A. Kool, B. Bagchi, P. Biswas, Md.M. Saikh, F. Khatun, S. Das, P.P. Ray, ACS Appl. Mater. Interfaces 9 (2017) 23048–23059.
[20] P. Thakur, A. Kool, B. Bagchi, N.A. Hoque, S. Das, P. Nandy, Phys. Chem. Chem. Phys. 17 (2015) 13082–13091.
[21] P. Martins, A.C. Lopes, S. Lanceros-Mendez, Prog. Polym. Sci. 39 (2014) 683–706.
[22] D.K. Das-Gupta, K.J. Doughty, Appl. Phys. 49 (1978) 4601–4603.
[23] J. Andrew, D. Clarke, Langmuir 24 (2008) 670–672.
[24] S.P. Bao, G.D. Liang, S.C. Tjong, Carbon 49 (2011) 1758–1768.
[25] D. Mandal, K. Henkel, D. Schmeißer, Mater. Lett. 73 (2012) 123–126.
[26] P. Thakur, A. Kool, B. Bagchi, S. Das, P. Nandy, Phys. Chem. Chem. Phys. 17 (2015) 1368–1378.
[27] P. Thakur, A. Kool, B. Bagchi, S. Das, P. Nandy, Appl. Clay Sci. 99 (2014) 149–159.
[28] J.-K. Yuan, S.-H. Yao, Z.-M. Dang, A. Sylvestre, M. Genestoux, J. Bai, J. Phys. Chem. C 115 (2011) 5515–5521.
[29] P. Thakur, A. Kool, B. Bagchi, N.A. Hoque, S. Das, P. Nandy, RSC Adv. 5 (2015) 28487–28496.
[30] T. Chen, L. Qiu, Z. Yang, Z. Cai, J. Ren, H. Li, H. Lin, X. Sun, H. Peng, Angew. Chem. 51 (2012) 11977–11980.
[31] Q. Wang, H. Chen, E. McFarland, L. Wang, Adv. Energy Mater. 5 (2015) 1–6.
[32] C.T. Chien, P. Hiralal, D.Y. Wang, I. Huang, C.C. Chen, C.W. Chen, G.A. Amaratunga, Small 11 (2015) 2929–2937.
[33] M. Zhang, Q.Q. Zhou, J. Chen, X.W. Yu, L. Huang, Y.R. Li, C. Li, G.Q. Shi, Energy Environ. Sci. 9 (2016) 2005–2010.
[34] J. Xu, Y. Chen, L. Dai, Nat. Commun. 6 (2015) 1–7.
[35] T.N. Murakami, N. Kawashima, T. Miyasaka, Chem. Commun. 26 (2005) 3346–3348.
[36] F. Zhou, Z. Ren, Y. Zhao, X. Shen, A. Wang, Y.Y. Li, C. Surya, Y. Chai, ACS Nano 10 (6) (2016) 5900–5908.
[37] G. Wee, T. Salim, Y.M. Lam, S.G. Mhaisalkar, M. Srinivasan, Energy Environ. Sci. 4 (2) (2011) 413–416.
[38] Z.L. Wang, J. Song, Science 312 (2006) 242–246.
[39] Y. Zhang, C. Liu, J. Liu, J. Xiong, J. Liu, K. Zhang, Y. Liu, M. Peng, A. Yu, A. Zhang, Y. Zhang, Z. Wang, J. Zhai, Z.L. Wang, ACS Appl. Mater. Interfaces 8 (2016) 1381–1387.
[40] S. Jana, S. Garain, S.K. Ghosh, S. Sen, D. Mandal, Nanotechnology 27 (2016) 1–12.
[41] M. Lee, C.-Y. Chen, S. Wang, S.N. Cha, Y.J. Park, J.M. Kim, L.-J. Chou, Z.L. Wang, Adv. Mater. 24 (2012) 1759–1764.
[42] M. Choia, G. Murillob, S. Hwanga, J.W. Kima, J.H. Junga, C.-Y. Chenc, M. Leea, Nano Energy 33 (2017) 462–468.
[43] X. Zhang, X. Huang, C. Li, H. Jiang, Adv. Mater. 25 (2013) 4093–4096.
[44] A.P. Indolia, M.S. Gaur, J. Polym. Res 43 (2013) 1–8.
[45] Q. Zhang, C.S. Dandeneau, X. Zhou, G. Cao, Adv. Mater. 21 (2009) 4087–4108.
[46] S.L. James, K.-Y. Shin, O.J. Cheong, J.H. Kim, J. Jang, Sci. Rep. 5 (2014) 1–6.
[47] S.K. Karan, R. Bera, S. Paria, A.K. Das, S. Maiti, A. Maitra, B.B. Khatua, Adv. Energy Mater. 6 (2016) 1–12.
[48] T.W. Dakin, IEEE Electr. Insul. Mag. 22 (2006) 11–28.
[49] N.A. Hoque, P. Thakur, N. Bala, A. Kool, S. Das, P.P. Ray, RSC Adv. 6 (2016) 29931–29943.
[50] X.B. Xu, S.H. Li, H. Zhang, Y. Shen, S.M. Zakeeruddin, M. Graetzel, Y.-B. Cheng, M.K. Wang, ACS Nano 9 (2015) 1782–1787.
[51] C. Shi, H. Dong, R. Zhu, H. Li, Y. Sun, D. Xu, Q. Zhao, D. Yu, Nano Energy 13 (2015) 670–678.
[52] M. Zhang, Q.Q. Zhou, J. Chen, X.W. Yu, L. Huang, Y.R. Li, C. Li, G.Q. Shi, Energy Environ. Sci. 9 (2016) 2005–2010.
[53] S. Hazebroucq, F. Labat, D. Lincot, C. Adamo, J. Phys. Chem. A 112 (2008) 7264–7270.
[54] F. Zhang, F. Shi, W. Ma, F. Gao, Y. Jiao, H. Li, J. Wang, X. Shan, X. Lu, S. Meng, J. Phys. Chem. C 117 (2013) 14659–14666.

Dr. Pradip Thakur is an Assistant Professor and the Head in Department of Physics, Netaji Nagar College for Women, Kolkata, India. He has acquired his Ph.D. in 2016 from the Department of Physics, Jadavpur University, India. Before that He completed his M.Sc. and B.Sc. in Physics in 2012 and 2010 respectively from the same university. His current research interest includes the development of advanced multifunctional materials, piezo-, pyro-, and ferro-electric polymers, synthesis and characterization of ceramic and metallic nanomaterials, designing of self-charging polymeric photo-power cells, fabrication of smart integrated devices for clean energy harvesting from living system and storage.

Dr. Arpan Kool has completed his Ph.D. from Department of Physics, Jadavpur University in 2017 and right now teaching physics in Techno India University, Kolkata. He received his M.Sc. and B.Sc. degree in physics from Jadavpur University in the year 2012 and 2010 respectively. His research is focussed on development of functional ceramic and polymer nano composites for multifunctional applications.

Mr. Nur Amin Hoque is currently pursuing his Ph.D. from the Department of Physics, Jadavpur University, India. He has obtained his M.Sc. and B.Sc. in Physics in 2013 and 2011 respectively from the same university. Fabrication of electroactive thin film polymer nanocomposites and exploring their application in the energy harvesting sectors such as piezoelectric nanogenerators, self-charging power cells are the realms of his research interests.

Dr. Biswajoy Bagchi has his research career based on developing ceramic and clay based functional nanocomposites for therapeutic and electro-ceramic applications. By undertaking a Masters in Biotechnology and a PhD research programme relating to Material Sciences from Jadavpur University, he has extended his research skills and expertise to involve Materials Science and Biology. He has diverse his experiences and skills in synthesis and characterization of metal nanoparticle, designing ceramic and polymer based antimicrobial bioceramics and smart devices for biomedical applications.

Mrs. Farha Khatun has obtained her M.Sc and B.Sc degree in physics from University of Calcutta, India in 2009 and 2011 respectively. Thereafter she has started PhD research work at Department of Physics, Jadavpur University, India. The PhD work is focussed on electroactive and high dielectric polymer composite based self-charging photo power cell.

Mr. Prosenjit Biswas is pursuing his Ph.D. from the Department of Physics, Jadavpur University, India. He has completed his M.Sc. and B.Sc. in Physics in 2016 and 2014 respectively from the same university. Synthesis of various nanoparticle, polymer composite films and simultaneous development of multifunctional polymeric power cell are his recent research interests.

Mr Debdip Brahma received his Bachelor of Science (B.Sc) and Master of Science degree in physics in 2014 and 2016 respectively from Jadavpur University. His research interest is in the area of experimental condensed matter physics.

Ms. Swagata Roy is presently pursuing her Ph.D. from the Department of Physics, Jadavpur University, India. She has completed her Masters and Bachelors in Physics in 2011 and 2009 respectively from the University of Burdwan, India. Her research interest chiefly focuses on the synthesis and development of electroactive polymer composite films and their application in piezo, pyro and solar energy harvesting arenas.

Ms. Somtirtha Banerjee has received her M.Sc and B.Sc degree in Microbiology from University of Calcutta, India in 2014 and 2012 respectively. She is pursuing PhD from Department of Physics, Jadavpur University, India. The research work is based on therapeutic application of ceramic and polymer materials.

Prof. Sukhen Das is a Professor in Department of Physics, Jadavpur University, India. He has acquired his Ph.D., M.Sc. (Physics) and B.Sc. (Physics) from the same university in 1995, 1990 and 1987 respectively. He has been working as a Scientist-B and Scientist-C in CGCRI, India in his initial years before joining Jadavpur University. He has guided several doctoral and post-doctoral fellows and has numerous research publications in reputed journals. Material science, nanoscience and therapy, development of ceramics, polymeric material and antimicrobial bio-ceramics and nanomaterials and their applicability in various potential sectors are the principle focus areas of his research.